SENP1 Knockdown Suppresses Tumor Progression in Lung Adenocarcinoma by Regulating AAR Genes Expression

Hong Cheng
National Cancer Center
Renda Li
National Cancer Center
Feng Wang
National Cancer Center
Xiangyang Yu
National Cancer Center
Feng Wang
National Cancer Center
Yi-Bo Gao (gaoyibo@cicams.ac.cn)
National Cancer Center/Cancer Hospital Chinese Academy of Medical Sciences https://orcid.org/0000-0002-0501-9814
Juwei Mu
National Cancer Center
Jie He
National Cancer Center

Research

Keywords: SUMO specific peptidase 1, lung adenocarcinoma, small ubiquitin-related modifier, amino acid transporter

Posted Date: May 7th, 2020

DOI: https://doi.org/10.21203/rs.3.rs-26420/v1

Abstract

Background SUMO specific peptidase 1(SENP1) is an important factor involved in the regulation of small ubiquitin-related modifier (SUMO) modification. Our previous research has shown that SENP1 could be a potential tumor-promoting factor in non-small cell lung cancer (NSCLC). However, its role in tumor progression remains largely unknown. This study aims to characterize the role of SENP1 in lung adenocarcinoma.

Methods The TCGA database provided us expression profiles of SENP1 and overall survival rates. loss-of-function assays were performed to examine the effect of SENP1 on proliferation, migration and invasion of lung adenocarcinoma cells in vitro and in vivo. Immunoprecipitation (IP), western blot and quantitative real time PCR (qRT-PCR) were carried out to reveal the interrelation between SENP1, SIRT6 and AAR (amino acid response) genes signal pathway.

Results In this study, we found that SENP1 was expressed at high levels in lung adenocarcinoma tissues and advanced TNM stages and was significantly associated with poor prognosis. we also found that SENP1 knockdown inhibited lung adenocarcinoma cell progression in vitro and in vivo. SUMOylation of SIRT6 was also observed in lung adenocarcinoma, and it was reduced by SENP1. SUMOylation of SIRT6 specifically increased its deacetylation of histone H3 on lysine 56 instead of that of lysine 9 (H3K9) in an in vitro model. Mechanistically, we found that knockdown of SENP1 reduced the expression of AAR genes by decreasing H3K56 acetylation through increasing SIRT6 SUMOylation. Moreover, mutation of the SUMOylation sites of Sirt6 reduced its tumor-suppressive effects.

Conclusions These results revealed that SENP1 promotion of tumor progression in lung adenocarcinoma and its tumor-promoting effects might be attributed to its important role in the regulation of Sirt6 SUMOylation and the expression of AAR genes.

Introduction

The morbidity and mortality associated with lung cancer are the highest in the world among malignant tumors[1]. It is known that lung cancer is a highly heterogeneous tumor. Lung cancer progression is characterized by a multistage and multistep process involving multiple genes and multiple factors. A large number of molecular abnormalities and mechanisms of action remain to be explored. Deep research examining the molecular level heterogeneity of lung cancer is a major challenge in basic and clinical research on lung cancer, and it is an important guide for the choice of individualized therapy for this disease and the search for novel targets for cancer therapy. Those research also contributes to the development of molecular diagnosis methods for lung cancer and promotes precision medicine for lung cancer treatment.

SUMOylation is a dynamic and reversible process in the development and progression of cancer. The SUMOylation of proteins results in different subcellular structures in eukaryotes. SUMOylation is mainly involved in the regulation of intracellular signal transduction, the cell cycle and apoptosis. Studies have

shown that protein SUMOylation, a process that relies on the interaction between the activating enzyme (E1), ligase (E2) and ligase (E3), is closely related to tumorigenesis. DeSUMOylation is catalyzed by a group of SUMO-specific protein (SENP) family members. The SENP family consists of six members: SENP1-3 and SENP5-7. The expression and activity of SENPs play important roles in the regulation of SUMOylation.

SENP1 is highly expressed in lung, prostate, pancreatic and thyroid cancers[2–4]. SENP1 can specifically enhance androgen receptor activity in prostate cancer[5], and the expression level of SENP1 is an independent prognostic factor for prostate cancer patients[6]. In B and T lymphocytic leukemia cells, SENP1 knockdown promotes cell cycle arrest, induces apoptosis, and inhibits cell proliferation. In our previous study, we analyzed the role of the SENP1 expression level in non-small cell lung cancer, and we found that SENP1 was highly expressed in cancer tissue compared with adjacent noncancerous tissue from patients with non-small cell lung cancer[7]. Patients with high expression of SENP1 are more inclined to develop acquired chemoresistance. High expression of SENP1 is also associated with a poor prognosis, indicating that SENP1 also plays an important role in the development of NSCLC (non-small cell lung cancer). However, the precise mechanism underlying the tumor-promoting effect of SENP1 in lung cancer remains to be elucidated.

We confirmed that SIRT6 (NAD + dependent histone deacetylase sirtuin-6) can be SUMOylated in mouse embryonic fibroblasts (MEFs). SIRT6 SUMOylation is mainly promoted by the interaction of SIRT6 and Myc, and increased SIRT6 is recruited to the promoter region of the Myc target genes to remove H3K56 acetylation modification, thereby reducing the expression of target genes to exert its tumor suppressor activity[8]. Our previous work also showed that SENP1 is highly expressed in non-small cell lung cancer specimens and is negatively correlated with chemosensitivity and prognosis. However, the detailed mechanisms of its functioning are still elusive. In this study, we explored the effect of abnormal SENP1 expression on the proliferation and invasion of lung cancer cells, including the effect of SENP1 on the level of SIRT6 SUMOylation and protein activity in lung adenocarcinoma. We aim to conduct the studies above to clarify the role of SENP1 in lung adenocarcinoma and its molecular mechanism, the possible use of SENP1 as a prognostic factor, and the therapeutic target in lung adenocarcinoma, thus promoting the precise treatment of lung cancer.

Methods

Database

The gene expression profiles of lung adenocarcinoma patients were obtained from The Cancer Genome Atlas (TCGA) database (https://tcga-data.nci.nih.gov/tcga/). Clinical characteristics such as gender, age, histological type, survival and outcome were also downloaded from the TCGA database. Kaplan-Meier plots were generated to illustrate the relationship between patient overall/progression-free survival and the gene expression levels of SENP1. The log-rank test was used to test the relationship.

Cell culture and stable cell line construction

Two cell lines were used in this study, H1299 and H1975. Lung adenocarcinoma cells were maintained in RPMI-1640 (HyClone) supplemented with 10% FBS (HyClone) and antibiotics (100 U/ml penicillin and 100 mg/ml streptomycin) (Invitrogen). Cell lines were cultured and maintained at 37 °C in a humidified atmosphere containing 5% carbon dioxide. We confirmed the cell line identities by comparing the short tandem repeat (STR) profile from each cell line to the registered information in the DSMZ online STR database.

Construction of cell Lines with stable knockdown of SENP1

The shRNA sequence was inserted into the pLKO.1 plasmid for viral packaging and infection to construct SENP1-silenced cell clones. The shRNA sequences were shRNA1, AACTACATCTTCGTGTACCTC, and shRNA2, CTAAACCATCTGAATTGGCTC. Lentivirus packaging and infection were performed as described previously[8]. Virus particles in cells were harvested after incubation for 48 h with Lipofectamine 3000 reagent (Invitrogen). H1299 and H1975 cells were infected with the recombinant lentivirus-transducing units and 5 mg/ml polybrene (Sigma-Aldrich) to increase the efficiency of infection.

Cell proliferation and Transwell assays

For the cell proliferation assay, treatment and control cells (3 × 103 cells/well) were plated in 96-well plates in complete serum medium. Cell viability was measured using the CCK-8 assay (Cell Counting Kit-8, Dojindo) according to the manufacturer's protocol. Cells (4 × 104 or 6 × 104) in serum-free RPMI 1640 medium were plated into the upper chamber of 24-well Transwell inserts (Corning, 8.0-μm pores) that were either uncoated or coated with Matrigel (Corning) for the migration or invasion assay, respectively. The cells were then allowed to migrate toward the RPMI-1640 containing 10% FBS for 24 h. Then, the cells on the lower side of the chamber were fixed, stained and counted in five different areas at 100x magnification.

Clone formation assay

To examine the clonogenic ability, cells were plated at 250 cells per well in 6-well culture dishes. Triplicate wells were performed for each group. Two weeks later, the cells were fixed in 4% paraformaldehyde (Servicebio, Wuhan) for 15 min and then stained with crystal violet (Beyotime, Shanghai) for 15 min. Clones with > 50 cells were scored, and the clone-formation ability was evaluated as the number of colonies.

Flow cytometry analysis of cell apoptosis

The Annexin V-PE/7-ADD kit (Becton Dickinson, BD) was used to analyzed the cell apoptosis according to the manufacturer's protocols. The cells were cultured in ultra-low attachment 6-well plates (Corning) for 24 hours. Then, the cells were harvested and washed with phosphate-buffered saline (PBS) twice, and then resuspended in 200 μl of binding buffer. Next, 5 μl of Annexin V-PE and 5 μl of 7-ADD were added and incubated for 15 min at room temperature in the dark. Flow cytometric analysis was then performed using a flow cytometer (FACSCalibur, BD, USA).

Nude mouse tumorigenesis experiment

A total of 8 BALB/c-nu mice (weight, 16–18 g; 4 males and 4 females; aged 4 weeks) were used in this study, The mice had free access to food and water, and they were maintained in a room at 20–22 °C with 40–70% humidity and a 12-h light/dark cycle. SENP1 knockdown and control cells (5 × 106) diluted in 0.1 ml PBS were injected subcutaneously into the left flank of the nude mice. Tumors appeared after approximately 12 days, and their dimensions were measured every 3 days using a digital caliper. The tumor volume was calculated as follows: V=(width2 × length)/2. Finally, the mice were sacrificed by carbon dioxide euthanasia, and the tumor weights were recorded.

Lung colonization assay

Female SCID-beige mice (aged 4 weeks) were used for the animal studies. The mice were divided into four groups and received tail-vein injections of 1 × 106 H1299 and H1975 cells containing different plasmids (shvec and sh1). After 1.5 months, the mice were sacrificed using CO2 anesthesia, and the number of tumor nodules on their lungs were counted after the excised tissues were paraffin-embedded, sectioned and stained with hematoxylin and eosin (H&E).

RNA extraction and quantitative real time PCR (qRT-PCR)

The relative RNA levels of genes were assessed by quantitative RT-PCR. Briefly, total RNA was isolated from cells with the standard TRIzol-based protocol (Tiangen, Beijing). The FastKing gDNA Dispelling RT SuperMix kit (Tiangen, Beijing) was used for reverse transcription. Real-time PCR was performed on an ABI 7900HT Real-Time PCR thermocycler (Life Technologies). Fold differences were calculated according to the $2-\Delta\Delta Ct$ method, and the endogenous control GAPDH (glyceraldehyde 3-phosphate dehydrogenase) was used to normalize the expression of the selected genes. The nucleotide sequences of the gene-specific primers were as follows: GAPDH (sense: 5′- CCT GGT ATG ACA ACG AAT TTG-3′, antisense: 5′- CAG TGA GGG TCT CTC TCT TCC-3′), SENP1 (sense: 5′- CAG CAG ATT TTA TCT TCC AGG C3′, antisense: 5′- CCC AAC TAT ATC TTG CAA GCA C-3′), TRIB3 (sense: 5′- CTA CGT GGG ACC TGA GAT ACT C-3′, antisense: 5′- GAG TCC TGG AAG GGG TAG T-3′), SLC1A4(sense: 5′-GAT CAG CAG GTT TAT TCT CCC C-3′, antisense: 5′- GAA TGG TGA AAA TCT GTC CTG C-3′), SLC1A5 (sense: 5′- CAG TCC TTG GAC TTC GTA AAG A-3′, antisense: 5′- CCA GGA TCA AGG AGA TAT GGT C-3′), SLC38A2 (sense: 5′- AGT TAT TTT CCC AAT CCG GAG T-3′, antisense: 5′- CTG TAA TGA GAC TAT GAC GCC A-3′).

Western blot analysis and immunoprecipitation

Total proteins were extracted using RIPA lysis buffer (Applygen, Beijing) and protease inhibitor (Thermo). Histones were extracted using the Histone Extraction kit (Abcam). Proteins were then separated by sodium dodecyl sulfate – polyacrylamide gel electrophoresis and transferred onto nitrocellulose filter membranes. After incubation with antibodies specific for human GAPDH (CST), H3 (CST), H3K9ac (CST), H3K27ac (CST), H3K56ac (CST), SENP1 (Abcam), SIRT6 (CST), the blots were incubated with HRP-conjugated second antibody for 1 h, and the bands detected using an ImageQuant LAS 4000 (GE).

SUMO-1 (Santa Cruz) conjugated to agarose was used for immunoprecipitation, which was performed strictly according to the kit instructions.

Statistical analysis

All statistical analyses were performed using SPSS software (version 20.0, Chicago, IL, USA). The Chi-squared test was used to analyze the relationship between SENP1 levels and the clinicopathological characteristics. Differences in SENP1 expression between groups were evaluated by the Mann-Whitney U test. The cell experimental results were presented as the means and S.E.M of three independent experiments, and the differences among groups were analyzed by the independent samples Student's t test. Differences were considered significant when $P < 0.05$.

Results

High SENP1 expression was significantly associated with poor survival in lung adenocarcinoma

We found that overexpression of SENP1 was associated with a lower tumor grade, higher T category, and higher TNM stage, and it was a promising predictor of poor survival according to immunohistochemistry of 100 NSCLC patient tissues in previous research. However, due to the small sample size, the results had a low confidence. Thus, we downloaded the expression profile of lung adenocarcinoma from TCGA, and we analyzed the association of SENP1 gene expression with the clinicopathological characteristics of lung adenocarcinoma. SENP1 was significantly upregulated in lung adenocarcinoma tumor tissues compared with normal tissues ($P < 0.001$, Fig. 1. A). SENP1 was significantly upregulated in lung adenocarcinoma tumor tissues compared with paired normal lung tissues ($P < 0.001$, Fig. 1. B). Compared with tumor tissues from patients with a lower T category (T1) or TNM stage (I), the tumor tissues of patients with a higher T category (T2-4) or TNM stage (II-IV) expressed higher levels of SENP1 ($P < 0.05$, Fig. 1. C-D). To determine whether SENP1 could affect prognosis, the Kaplan–Meier survival curve and log-rank test were used, which showed that decreased expression of SENP1 was significantly associated with improved overall survival ($p = 0.0136$, Fig. 1. E) and progression-free survival ($p = 0.0181$, Fig. F) in patients.

SENP1 knockdown inhibited the proliferation, migration, and invasion of lung adenocarcinoma cells in vitro

We further investigated the biological function of SENP1 in lung adenocarcinoma cells. The expression of SENP1 was markedly decreased after transfection with two specific SENP1 shRNAs (sh1 and sh2) compared with the mock-vehicle control in H1975 and H1299 cells (Fig. 2. A). The downregulation of SENP1 significantly decreased the proliferation, migration and invasion ability of H1975 and H1299 cells compared with the mock-vehicle control (Fig. 2. B-C). In addition, compared with the mock-vehicle control, decreased expression of SENP1 resulted in a significant decrease in cell clone forming ability in H1975 and H1299 cells (Fig. 2. D). These results showed that SENP1 knockdown negatively regulated the proliferation, migration, invasion and clone-formation ability of lung adenocarcinoma cells.

SENP1 knockdown inhibited the proliferation and metastasis of lung adenocarcinoma cells in vivo

To further evaluate the tumor-promoting effect of SENP1 in lung adenocarcinoma, tumors were resected from tumor-bearing mice and measured (Fig. 3. A), and their weight and volume were significantly lower in the SENP1 knockdown group compared with the control group ($P < 0.001$; Fig. 3. B). Knockdown of SENP1 exerted a significant inhibitory effect on tumor volume in vivo compared with the control group ($P < 0.001$; Fig. 3. C). Then, SENP1-knockdown H1299 and H1975 cells were injected into the tail veins of nonobese diabetic nude mice. We calculated the number of pulmonary metastatic nodules in mice 1.5 months after caudal intravenous injection. Mice injected with cells with silenced SENP1 showed lower rates of lung colonization and less metastatic tumor nodules in the lung than mice injected with control cells (Fig. 3. D). Images of H&E-stained lung tissue samples isolated from mice are illustrated in Figure.

SENP1 inhibited SUMOylation of Sirt6 and promoted H3K56 acetylation.

First, we found that SIRT6 could be SUMOylated in lung adenocarcinoma (Fig. 4. A), which was consistent with our previous study[7]. SENP1 is the specific enzyme for SIRT6 deSUMOylation, and knockdown of SENP1 could increase the SUMOylation level of SIRT6 (Fig. 4. B). It is well known that SIRT6 mainly deacetylates chromatin marks at histone H3 lysine 9 (H3K9) and 56 (H3K56)[9], and we finally found that SENP1 knockdown could decrease the acetylation of H3K56 instead of H3K9 or H3K27, indicating that the SUMOylation of SIRT6 selectively promoted its function in H3K56 acetylation(Fig. 4. C). To further study the physiological function of the SUMOylation of SIRT6, we established two stable SIRT6-knockdown lung adenocarcinoma cell lines (Fig. 4. D). We had previously constructed the wild-type and mutant-type plasmids of SIRT6[9]. Next, to better compare the differences between wild-type SENP1 and the mutants, stable cell lines overexpressing wild-type SIRT6 and the mutant were successfully generated in H1299 and H1975 cells (Fig. 4. E). As expected, mutation of the SUMOylation sites of SIRT6 mainly changed the function of SIRT6 in the deacetylation of chromatin marks at H3K56 instead of at H3K9 (Fig. 4. F). Finally, mutation of the SUMOylation sites of SIRT6 partially reversed the SIRT6-induced inhibition of tumor promotion in lung adenocarcinoma in the clone formation assay (Fig. 4. G-H). Collectively, all these results suggested that SENP1 regulated tumor promotion in lung adenocarcinoma through the SIRT6/H3K56ac pathway. To further define the function of SIRT6 SUMOylation in the SENP1 effect, Si-SENP1 was used to knockdown SENP1 based on the wild-type and mutant-type SIRT6 overexpression. Compared with the overexpression of the wild-type SIRT6, SENP1 knockdown could hardly reduce the SIRT6 function of deacetylating H3K56 with overexpression of the mutants (Fig. 4. I). The clone-formation ability with wild-type SIRT6 overexpression was clearly recued compared with the mutants through si-SENP1 (Fig. 4. J). The results described above all show that SIRT6 SUMOylation plays an important role in the SENP1 tumor-promoting effect.

SENP1 regulated the expression of AAT genes.

To further define the function of SIRT6 SUMOylation in the SENP1 effect, Transcriptome sequencing (RNA-seq) was performed to investigate expression profiles of SENP1 knockdown group and the control group. SENP1 mRNA expression was successfully knocked down by shRNA(Fig. 5. A). The amino acid

response (AAR) genes associated with the ATF4-dependent transcriptional mechanisms were down-regulated by the knockdown of SENP1, such as ASNS, TRIB3, SLC38A2(Fig. 5. B). Then, The expression of ASNS, TRIB3, SLC38A2,SLC1A4 and SLC1A5 was verified via qRT-PCR, using β-actin as a reference gene(Fig. 5. C). We next analyzed the expression of AAR genes in the cells with wild-type SIRT6 overexpression and the mutants through qRT-PCR, The AAR genes with wild-type SIRT6 overexpression was clearly recued compared with the mutants(Fig. 5. D). The results described above all show that SIRT6 SUMOylation plays an important role in the regulation of AAR genes. As ATF4 play an important role in response to amino acid starvation or ER stress, the relative cell survival rate was determined by CCK-8 assay under glucose or glutamine deprivation. Compared with the control group cells, the survival rate of SENP1 knockdown group was significantly reduced (Fig. 5. E). And SENP1 knockdown increased apoptosis of cells in suspension culture for 24 h(Fig. 5. F).To further confirm the above results, Spearman correlation analysis was used to disclose the correlation between SENP1 and AAR genes in the expression profile of lung adenocarcinoma from the TCGA database. There was a significant positive correlation between SENP1 and AAR genes (Fig. 6. A). And we found AAR genes such as ASNS, TRIB3, SLC38A2, SLC1A5 were the prognosticators of poor survival in lung adenocarcinoma by using the TCGA database(Fig. 6. B-I). Taken together, these results suggest AAR genes may be the key factor regulating tumor progression by SENP1.

Discussion

SENP1 plays an important role in many cancers, The expression level of SENP1 in prostate cancer and the prognosis of patients is significantly correlated[6]. We have previously studied the relationship between SENP1 expression and non-small cell lung cancer, and we found that patients with high expression of SENP1 have a poor prognosis. SENP1 expression has shown an abnormal association in the development of non-small cell lung cancer; this finding has not been verified in a larger sample. In our study, we verified the above conclusions and found a lower expression level of SENP1 in early stages (TNM stage I) compared with that in advanced stages (TNM stage II and IV) of lung adenocarcinoma, and higher expression predicted poor overall and progression-free survival. However, Verification of these findings in tissue specimens or clinical patients is necessary in further study.

Knockdown of SENP1 suppresses cell proliferation and transformation in breast cancer cell lines[11]. SENP1 regulates cell apoptosis in prostate epithelia.[12] The low levels of SENP1 were essential for the maintenance of stemness in osteosarcoma stem cells, and SENP1 overexpression led to a significant increase in the sensitivity of osteosarcoma stem cells to the herpes simplex virus 1 thymidine kinase gene in combination with ganciclovir in vitro and in vivo. SENP1 plays an important role in regulating genes that are important for cancer development and progression[13]. It can affect cancer-related processes such as cellular proliferation and invasion[5, 14]. In our study silencing of SENP1 expression in H1299 and H1975 obviously decreased the cell viability, migration and invasion ability, and colony-formation ability In vitro and in vivo. In general, SENP1 promoted tumor progression .

SENP1 exerts its actions through a multiplicity of mechanisms.SENP1 can decrease PTEN protein stability by regulating PTEN SUMOylation and ubiquitylation. It also modulates cell apoptosis in prostate epithelia[11]. Overexpression of SENP1 has been shown to regulate glycolysis in prostatic carcinoma cells by stabilizing HIF1α[14]. SENP1 was been found to be a crucial c-Myc deSUMOylating enzyme that positively regulates c-Myc stability and activity in breast cancer[11]. In our study, SIrt6 could be SUMOylated in lung adenocarcinoma, and the mutation of SUMOylation sites in Sirt6 decreased its tumor-suppressive activity. Additionally, knockdown of SENP1 promoted Sirt6 SUMOylation in lung adenocarcinoma. We found that the mutation of SUMOylation sites in Sirt6 could offset the effect of SENP1 knockdown to some extent. In conclusion, we found that SENP1 plays an important role in lung adenocarcinoma by deSUMOylating Sirt6.

SIrt6 is an important tumor suppressor gene, which deacetylates chromatin marks at histone H3 lysine 9 (H3K9) and 56 (H3K56)[10]. Sirt6 can repress the transactivation of several transcription factors by modulating these two acetylation markers of histone H3[15]. In our previous research, Sirt6 was found to be a SUMOylated protein, but few studies have examined SIRT6 and SUMOylation in lung adenocarcinoma. We also found that Sirt6 was a SUMOylated protein in lung adenocarcinoma. Additionally, Sirt6 SUMOylation could promote its tumor-suppressive activity, and Sirt6 SUMOylation deficiency did not affect its deacetylation activity on H3K9 but almost completely abolished its deacetylation of H3K56. Sirt6 can co-repress MYC transcriptional activity and the expression of ribosomal genes. In our previous study, Sirt6 SUMOylation modulated its suppression of ribosome biogenesis genes such as Rpl3, Rpl6, Rpl23 and Rps15a[8]. In contrast, SIRT6 also acts as a corepressor of several transcription factors that are implicated in glucose and lipid metabolism[16]. SIRT6 is recruited to amino acid transporter(AAT) promoters by interactions with ATF4, deacetylates histone H3K56, destabilizes ATF4 from chromatin, and leads to repression of the AAT gene expression[17]. In our study, there were no differences in these ribosome biogenesis genes in the SENP1 knockdown group and nc group. In contrast, knockdown of SENP1 could decrease the expression of AAR genes. Collectively, these findings indicate that the tumor-promoting effect of SENP1 occurs via increased expression of AAR genes through the SUMOylation of Sirt6.

Activating transcription factor 4 (ATF4) act as a stress-induced transcription factor which is often upregulated in multiple cancers. ATF4 controll the expression of a range of genes that allow cells to survive when exposed to stresses, such as amino acid limitation [18]. And Tumor cells are usually in the state of nutritional deficiency. ATF4 activates AAR genes such as ASNS, TRIB3, SLC38A2 via a C/EBP-ATF response element (CARE) [19], and AAR genes play a key role in glutamine uptake and metabolism [20]. Glutamine is a key nitrogen-based substrate for nucleotide and amino acid biosynthesis in rapidly proliferating cancer cells[21]. Increased loss of Gln results in its selective depletion in tumor tissues. Additionally, the core region of solid tumors is more inclined to show Gln deficiency[22]. In addition, spatial examination of amino acid levels in cancer cell xenografts has shown that glutamine is most depleted in the xenograft core when compared to cells in the tumor interior[22]. In our study, tumors with high SENP1 expression tended to be larger, potentially due to the higher AAT gene expression. Glutamine also plays an important role in redox control. Tumor cells encounter oxidative stress during their

progression, metastatic colonization, and following exposure to anti-tumor drugs, which increases their dependence on antioxidative responses[23]. Products of glutamine metabolism play a significant role in facilitating cellular anti-oxidative defense. First, glutamine-derived glutamate is utilized in the de novo biosynthesis of glutathione, a primary cellular antioxidant [24]. Second, glutamine-derived glutamate contributes to glutathione biosynthesis through facilitating the uptake of cystine via the xCT transporter. Third, glutamine contributes to the cellular redox balance by supporting NADPH production[25] [27]. SENP1 played an important role in regulating cancer development and progression in our study, These observations might be correlated with the ability of glutamine to better cope with stresses, especially oxidative stress. AAR genes are potential cancer therapeutic targets.

Given the important role of SENP1 in cancer progression, compounds that selectively inhibit SENP1 have shown great prospects in tumor therapy. In-silico screening was used to search for small molecule inhibitors of SENP1 in conjunction with biochemical assays, and a new chemotype of small molecule inhibitors that noncovalently inhibit SENP1 was found and the inhibitory abilities of representative inhibitors of SENP1 in cells confirmed in HELA cells[26]. Hinokiflavone, which belongs to a subclass of the plant flavonoid family, could have a similar effect through its ability to block SENP1 activity and therefore stimulate the accumulation of hyper-SUMOylated proteins to inhibit cancer progression[27].

Overall, these findings suggest the potential of SENP1 as a therapeutic target in cancer. Moreover, based on our research, AAR genes might be key factors regulating tumor progression by SENP1 in lung adenocarcinoma, And a high level of glutamine was anticipated in tumors with SENP1 overexpression. Glutamine metabolism is considered a new therapeutic target, and a number of glutamine-mimetic compounds, including 6-diazo-5-oxo-L-norleucine (DON), acivicin, and azaserine, have been evaluated in preclinical and clinical settings for their anti-tumor activities[21]. Due to its potential contribution to tumor adaptated to microenvironmental stress, drug resistance and metastasis, AAR genes are considered to be interesting targets for cancer treatment [18]. In general, the expression of SENP1 might be an important factor in the selection of inhibitors of glutamine metabolism. Further studies are needed to determine the effect of SENP1 on cellular metabolism.

Conclusion

In summary, the present study revealed SENP1 promotion of tumor progression in lung adenocarcinoma, which might be attributed to its important role in the regulation of Sirt6 SUMOylation and the expression of AAR genes. These findings of the in vitro and in vivo experiments provide an important contribution to knowledge of the regulatory mechanisms of SUMOylation in tumor progression. Moreover, in view of the high expression of SENP1 in lung adenocarcinoma tumor tissues and its independent prognostic significance, our study confirmed that SENP1 is a good biomarker for lung adenocarcinoma prognosis as well as a potential drug target for lung adenocarcinoma treatment.. However, verification of these findings in tissue specimens is necessary in further investigations, and the underlying mechanism needs to be studied further.

Abbreviations

AAR
amino acid response
AAT
amino acid transporter
ATF4
activating transcription factor 4
CCK-8
Cell counting kit-8
IP
Immunoprecipitation
FBS
Fetal bovine serum
NSCLC
Non-small cell lung cancer
PBS
Phosphate Buffered Saline
SUMO
small ubiquitin-related modifier
SENP1
SUMO specific peptidase 1

Declarations

Acknowledgements

Not applicable.

Funding

The work was supported by the National Natural Science Foundation of China (81672306), the Beijing Municipal Natural Science Foundation (7171007).

Availability of data and materials

The datasets used and/or analyzed during the current study are available from the corresponding author on reasonable request.

Authors' contributions

HC carried out the experiments and drafted the manuscript; RL contributed to the RT-qPCR experiments; XY and FW contributed to western blot assay; FW were involved in the statistical analysis; YG critically reviewed the manuscript; JM and JH managed the experimental design, reviewed the manuscript and provided funding support. All authors read and approved the final manuscript.

Competing interests

The authors declare that they have no competing interests.

Ethics approval and consent to participate

This study was approved by the Ethics Committee of National Cancer Center/Cancer Hospital, Chinese Academy of Medical Sciences and Peking Union Medical College (Beijing, China).

References

1. Torre LA, Bray F, Siegel RL, Ferlay J, Lortet-Tieulent J, Jemal A. Global cancer statistics, 2012. Cancer J Clin. 2015;65:87–108.
2. Jacques C, Baris O, Prunier-Mirebeau D, Savagner F, Rodien P, Rohmer V, et al. Two-step differential expression analysis reveals a new set of genes involved in thyroid oncocytic tumors. J Clin Endocrinol Metab. 2005;90:2314–20.
3. Wang C, Tao W, Ni S, Chen Q, Zhao Z, Ma L, et al. Tumor-suppressive microRNA-145 induces growth arrest by targeting SENP1 in human prostate cancer cells. Cancer Sci. 2015;106:375–82.
4. Ma C, Wu B, Huang X, Yuan Z, Nong K, Dong B, et al. SUMO-specific protease 1 regulates pancreatic cancer cell proliferation and invasion by targeting MMP-9. Tumour Biol. 2014;35:12729–35.
5. Zhang X, Wang H, Wang H, Xiao F, Seth P, Xu W, et al. SUMO-Specific Cysteine Protease 1 Promotes Epithelial Mesenchymal Transition of Prostate Cancer Cells via Regulating SMAD4 deSUMOylation. International journal of molecular sciences. 2017; 18.
6. Wang Q, Xia N, Li T, Xu Y, Zou Y, Zuo Y, et al. SUMO-specific protease 1 promotes prostate cancer progression and metastasis. Oncogene. 2013;32:2493–8.
7. Mu J, Zuo Y, Yang W, Chen Z, Liu Z, Tu J, et al. Over-expression of small ubiquitin-like modifier proteases 1 predicts chemo-sensitivity and poor survival in non-small cell lung cancer. Chin Med J. 2014;127:4060–5.

8. Cai J, Zuo Y, Wang T, Cao Y, Cai R, Chen FL, et al. A crucial role of SUMOylation in modulating Sirt6 deacetylation of H3 at lysine 56 and its tumor suppressive activity. Oncogene. 2016;35:4949–56.
9. Lu Z, Li Y, Che Y, Huang J, Sun S, Mao S, et al. The TGFbeta-induced lncRNA TBILA promotes non-small cell lung cancer progression in vitro and in vivo via cis-regulating HGAL and activating S100A7/JAB1 signaling. Cancer Lett. 2018;432:156–68.
10. Kugel S, Mostoslavsky R. Chromatin and beyond: the multitasking roles for SIRT6. Trends Biochem Sci. 2014;39:72–81.
11. Sun XX, Chen Y, Su Y, Wang X, Chauhan KM, Liang J, et al. SUMO protease SENP1 deSUMOylates and stabilizes c-Myc. Proc Natl Acad Sci U S A. 2018;115:10983–8.
12. Bawa-Khalfe T, Yang FM, Ritho J, Lin HK, Cheng J, Yeh ET. SENP1 regulates PTEN stability to dictate prostate cancer development. Oncotarget. 2017;8:17651–64.
13. Liu F, Li L, Li Y, Ma X, Bian X, Liu X, et al. Overexpression of SENP1 reduces the stemness capacity of osteosarcoma stem cells and increases their sensitivity to HSVtk/GCV. Int J Oncol. 2018;53:2010–20.
14. Wang C, Tao W, Ni S, Chen Q. SENP1 Interacts with HIF1alpha to Regulate Glycolysis of Prostatic Carcinoma Cells. Int J Biol Sci. 2019;15:395–403.
15. Toiber D, Erdel F, Bouazoune K, Silberman DM, Zhong L, Mulligan P, et al. SIRT6 recruits SNF2H to DNA break sites, preventing genomic instability through chromatin remodeling. Molecular cell. 2013;51:454–68.
16. Tasselli L, Zheng W, Chua KF. SIRT6: Novel Mechanisms and Links to Aging and Disease. Trends Endocrinol Metab. 2017;28:168–85.
17. Zhang N, Yang X, Yuan F, Zhang L, Wang Y, Wang L, et al. Increased Amino Acid Uptake Supports Autophagy-Deficient Cell Survival upon Glutamine Deprivation. Cell Rep. 2018;23:3006–20.
18. Wortel IMN, van der Meer LT, Kilberg MS, van Leeuwen FN. Surviving Stress: Modulation of ATF4-Mediated Stress Responses in Normal and Malignant Cells. Trends Endocrinol Metab. 2017;28(11):794–806.
19. Kilberg MS, Shan J, Su N. ATF4-dependent transcription mediates signaling of amino acid limitation. Trends Endocrinol Metab. 2009;20(9):436–43.
20. Hu X, Deng J, Yu T, Chen S, Ge Y, Zhou Z, et al. ATF4 Deficiency Promotes Intestinal Inflammation in Mice by Reducing Uptake of Glutamine and Expression of Antimicrobial Peptides. Gastroenterology. 2019;156(4):1098–111.
21. Zhang J, Pavlova NN, Thompson CB. Cancer cell metabolism: the essential role of the nonessential amino acid, glutamine. Embo j. 2017;36:1302–15.
22. Pan M, Reid MA, Lowman XH, Kulkarni RP, Tran TQ, Liu X, et al. Regional glutamine deficiency in tumours promotes dedifferentiation through inhibition of histone demethylation. Nat Cell Biol. 2016;18:1090–101.

23. Gorrini C, Harris IS, Mak TW. Modulation of oxidative stress as an anticancer strategy. Nat Rev Drug Discov. 2013;12:931–47.
24. Lu SC. Regulation of glutathione synthesis. Mol Aspects Med. 2009;30:42–59.
25. Son J, Lyssiotis CA, Ying H, Wang X, Hua S, Ligorio M, et al. Glutamine supports pancreatic cancer growth through a KRAS-regulated metabolic pathway. Nature. 2013;496:101–5.
26. Madu IG, Namanja AT, Su Y, Wong S, Li YJ, Chen Y. Identification and characterization of a new chemotype of noncovalent SENP inhibitors. ACS Chem Biol. 2013;8:1435–41.
27. Pawellek A, Ryder U, Tammsalu T, King LJ, Kreinin H, Ly T, et al. Characterisation of the biflavonoid hinokiflavone as a pre-mRNA splicing modulator that inhibits SENP. eLife. 2017; 6.

Figures

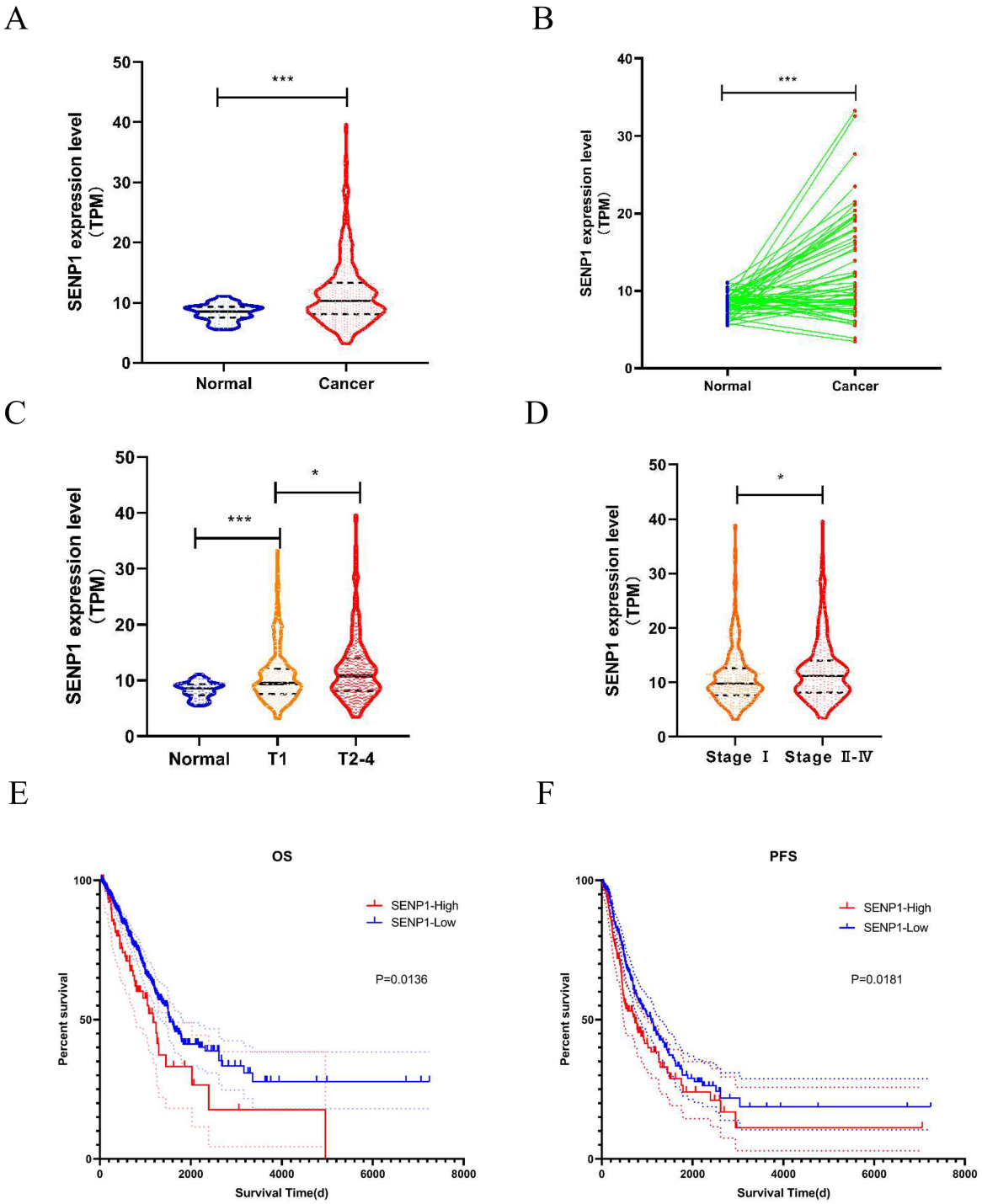

Figure 1

Aberrant expression of SENP1 in lung adenocarcinoma samples. (A) The relative SENP1 expression (TPM) in 513 tumor tissues was compared with 59 adjacent noncancerous lung tissues. (B) SENP1 expression (TPM) in 59 tumor tissues was compared with that in paired adjacent noncancerous lung tissues. (C) The relative expression of SENP1 (TPM) was compared between 342 patients with advanced T stages (2-4) and 168 patients with early T stages. (D) The relative expression of SENP1 (TPM) was

compared between 231 patients with advanced stages (Ⅱ-Ⅳ) and 274 patients with early T stages (Ⅰ). (E) Kaplan–Meier survival analysis of overall survival in 490 lung adenocarcinoma patients. The two-tailed Student's t-test was used. (F) Kaplan–Meier survival analysis of progression-free survival in 462 lung adenocarcinoma patients. The data are shown as the mean ± SD, *p < 0.05, **p < 0.01, ***p < 0.001.

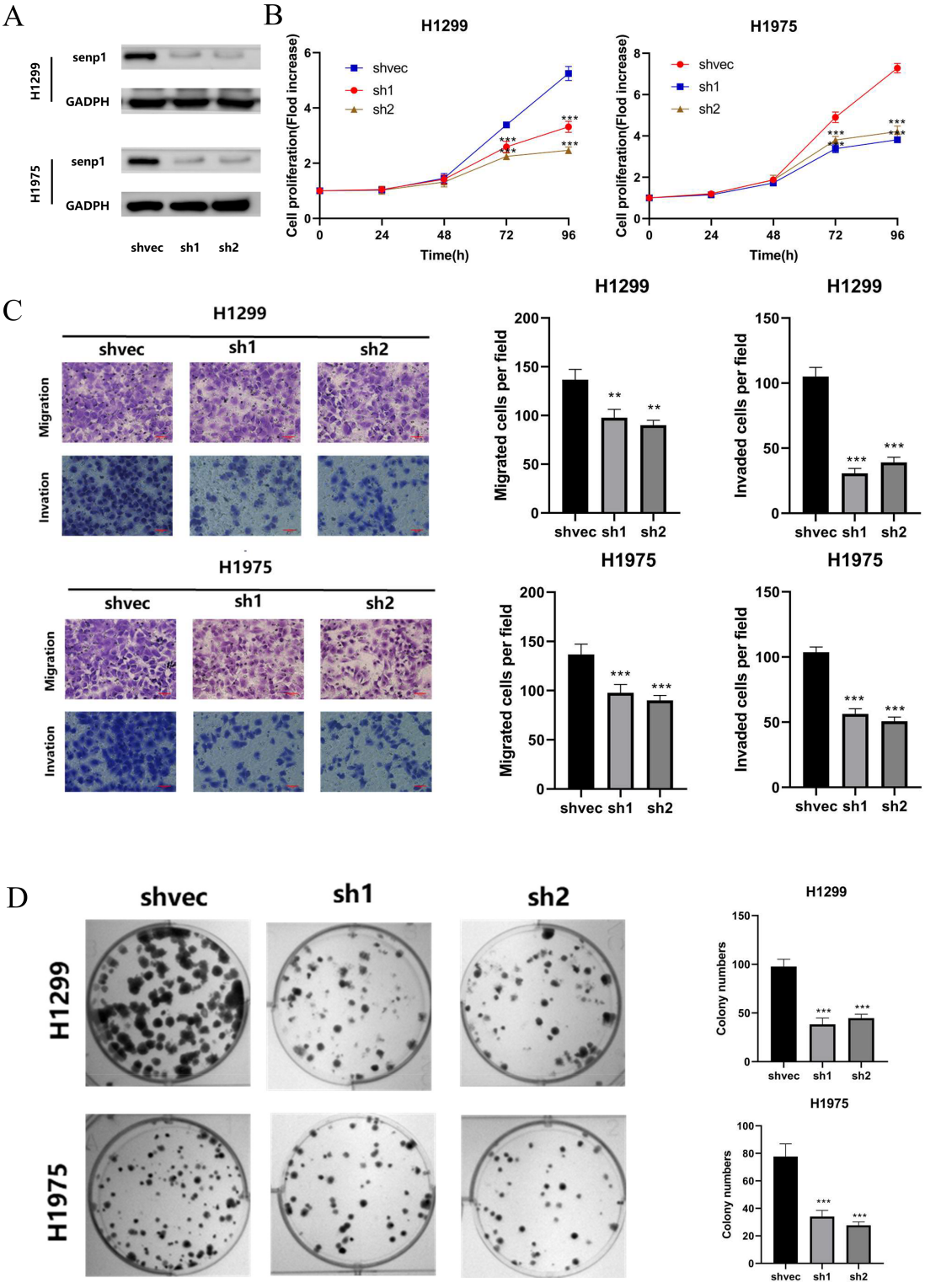

Figure 2

SENP1 knockdown inhibited lung adenocarcinoma cell progression in vitro. (A) The expression level of SENP1 by Western blotting in stable SENP1 knockdown or mock vehicle control-transfected H1975 and H1299 cell lines, GADPH was used as a loading control. (B)The proliferation ability of SENP1 knockdown or mock vehicle control-transfected H1975 and H1299 cell lines, as detected by the CCK-8 assay. (C) The migration and invasion ability of SENP1 knockdown or mock vehicle control-transfected H1975 and H1299 cell lines, as detected by the transwell assay. The numbers of migrating and invading cells were compared between the groups. (D) The colony-forming ability of SENP1 knockdown or mock vehicle control-transfected H1975 and H1299 cell lines, as detected by the clone formation assay. The numbers of colony were compared between the groups. The data are shown as the mean ± SD, *p < 0.05, **p < 0.01, ***p < 0.001.

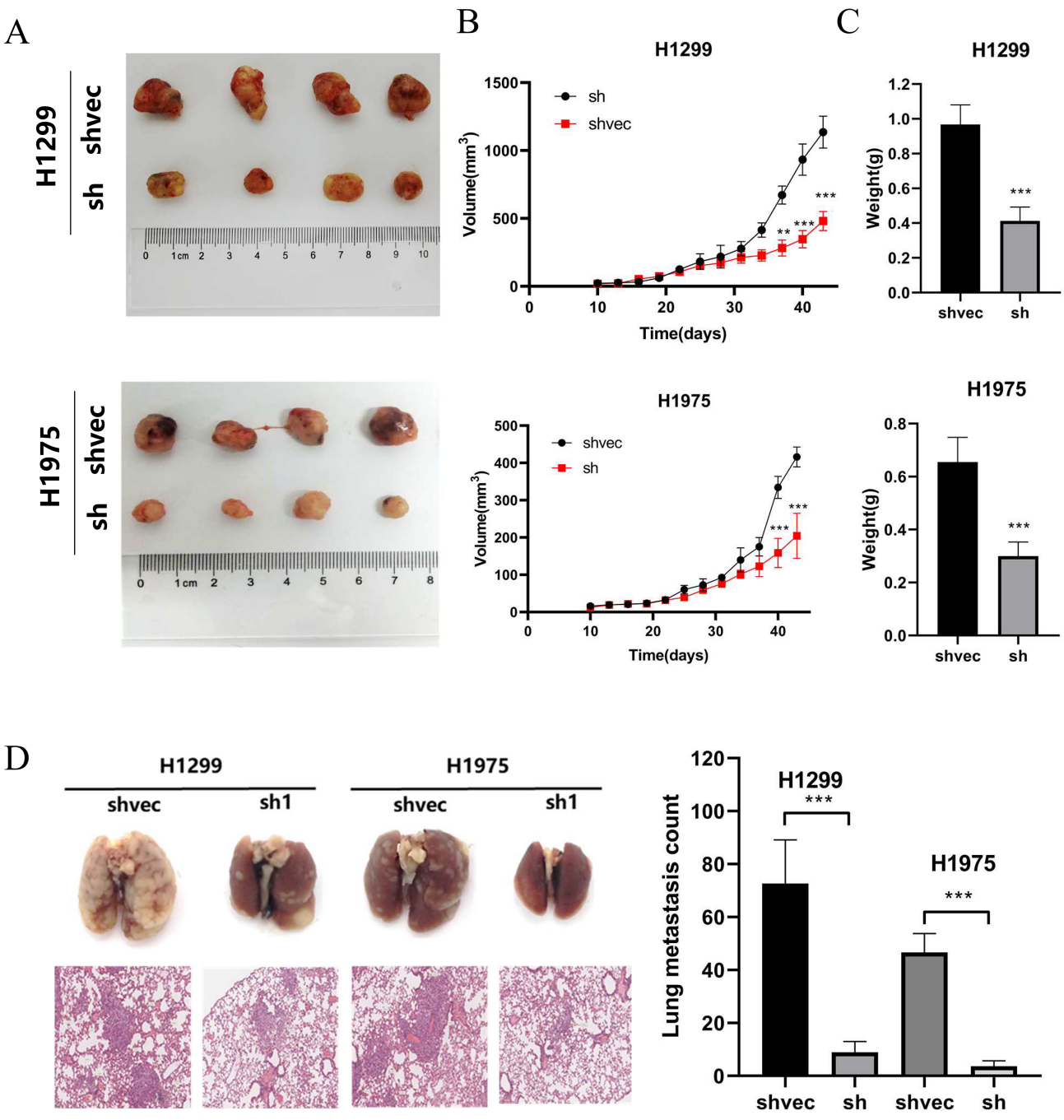

Figure 3

SENP1 knockdown inhibited lung adenocarcinoma cell progression in vivo. (A) Representative images of tumor tissues isolated from mice injected with 1 × 106 H1975 and H1299 cell lines into the left flank. The tumor volumes and tumor weights were compared between the groups. (B) Representative images of lung tissues isolated from mice injected with 1 × 106 H1975 and H1299 cell lines via the tail vein and hematoxylin and eosin-stained images (100×) of these tissues. The number of metastatic nodules in the lung were compared between the groups. The data are shown as the mean ± SD, *p < 0.05, **p < 0.01, ***p < 0.001.

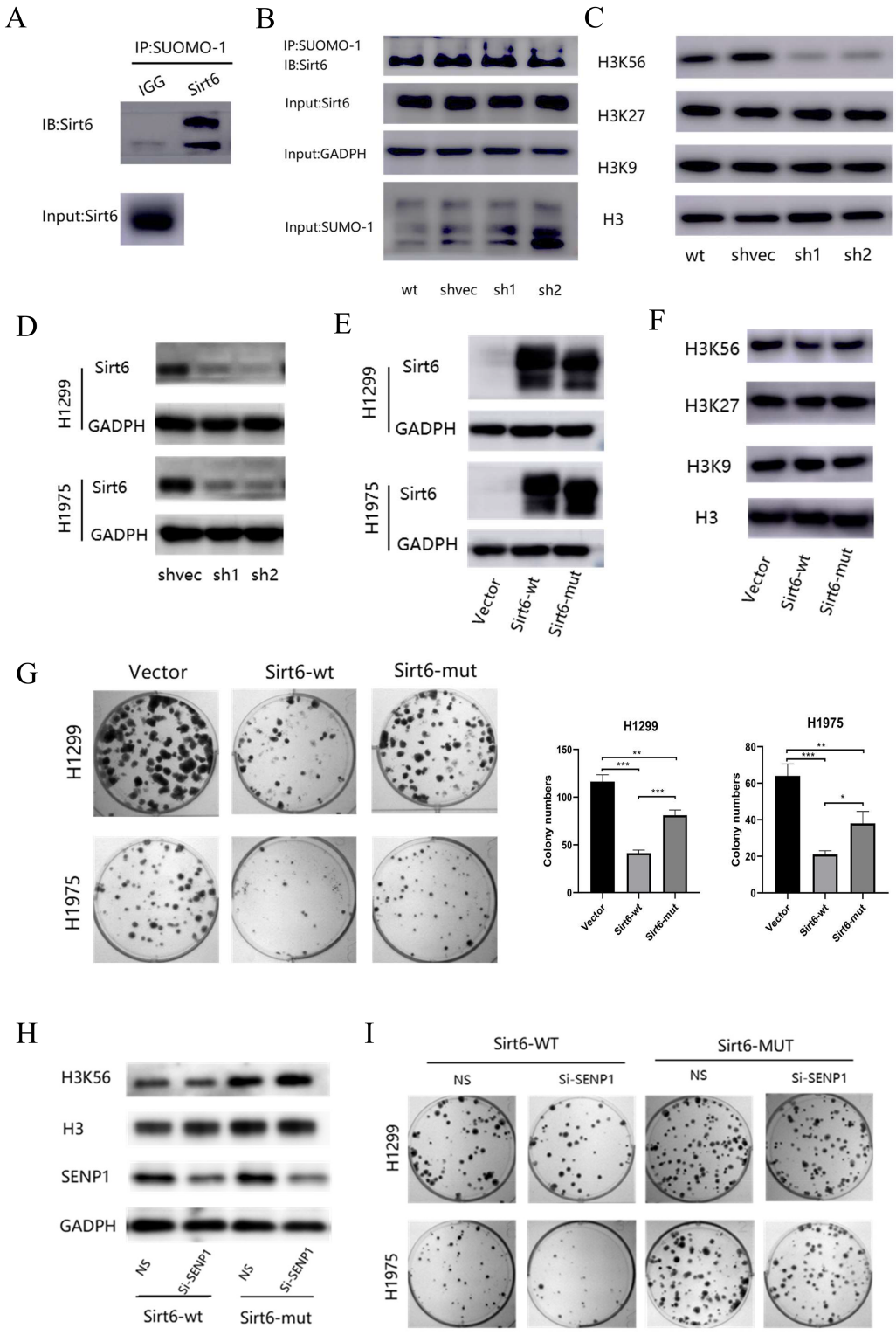

Figure 4

SENP1 inhibited SUMOylation of Sirt6 and promoted H3K56 acetylation (A) Endogenous SUMOylation of Sirt6. Protein fractions extracted from 1 × 107 H1299 cells were immunoprecipitated with anti-SUMO1 or anti-IgG antibodies. The IPs were immunoblotted with anti-Sirt6 (CST) antibodies. (B) Protein fractions extracted from stable SENP1 knockdown or mock vehicle control-transfected H1975 cell lines with anti-SUMO1 or anti-IgG antibodies. The IPs were immunoblotted with anti-Sirt6 (CST) antibodies. (C) Western

blotting showing H3, H3K9, H3K27, and H3K56 in stable SENP1 knockdown or mock vehicle control-transfected H1975 cells. GAPDH was used as the loading control. (D) Western blotting showing Sirt6 in stable Sirt6 knockdown or mock vehicle control-transfected H1975 and H1299 cells. GAPDH was used as the loading control. (E) Western blotting showing Sirt6 in stable Sirt6 WT, Sirt6 MUT or mock vehicle-transfected H1975 and H1299 cells. GAPDH was used as the loading control. (F) Western blotting showing H3, H3K9, H3K27, and H3K56 in stable Sirt6 WT, Sirt6 MUT or mock vehicle -transfected H1299 cells. GAPDH was used as the loading control. (G) The colony-forming ability of stable Sirt6 WT, Sirt6 MUT or mock vehicle-transfected H1299 and H1975 cells, as detected by the clone formation assay. The numbers of colonies were compared between the groups. (H) Western blotting showing SENP1 and H3K56 in H1299 cells transfected with Sirt6 WT or Sirt6 MUT plus SENP1 siRNA. (I) The colony-forming ability of H1299 cells transfected with Sirt6 WT or Sirt6 MUT plus SENP1 siRNA, as detected by the clone formation assay. The numbers of colonies were compared between the groups

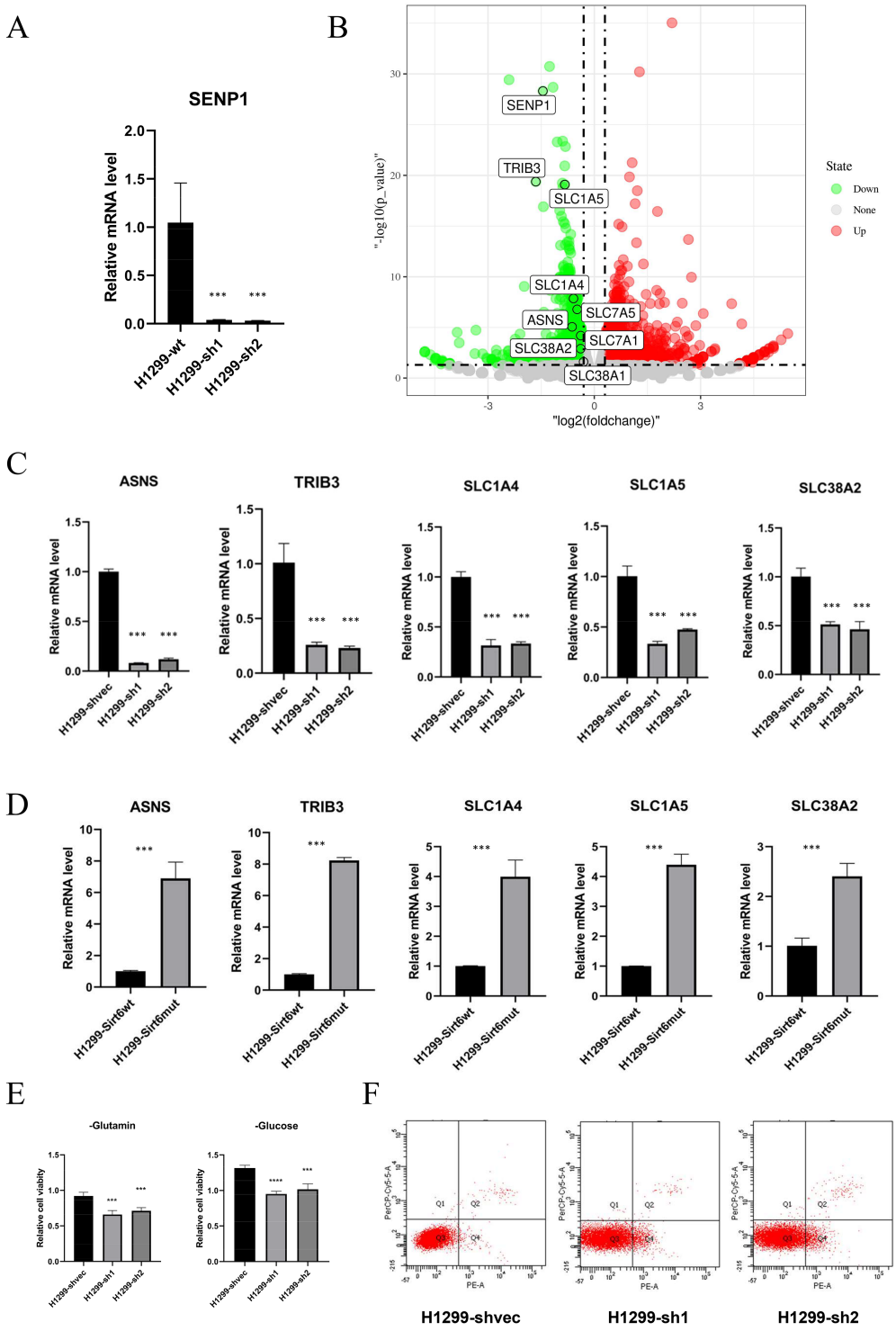

Figure 5

SENP1 regulated the expression of AAR genes. (A) Real-time PCR was used to analyze the mRNA levels of the SENP1 in stable SENP1 knockdown or mock vehicle control-transfected H1299 cell lines (B) The volcano map of differentially expressed genes in stable SENP1 knockdown or mock vehicle control-transfected H1299 cell lines in the transcriptome sequencing results. In this volcano map, upregulated genes are presented as red dots and downregulated genes as green dots. (C) Real-time PCR was used to

analyze the mRNA levels of the ATF4 target genes ASNS, TRIB3, SlC1A4, SLC1A5, and SLC38A2 in stable SENP1 knockdown or mock vehicle control-transfected H1299 cell lines. (D) Real-time PCR was used to analyze the mRNA levels of the ATF4 target genes ASNS, TRIB3, SlC1A4, SLC1A5, and SLC38A2 in stable Sirt6 WT, Sirt6 MUT or mock vehicle-transfected H1299 and H1975 cells. (E) The relative cell survival rate was determined by CCK-8 assay under glucose or glutamine deprivation in stable SENP1 knockdown or mock vehicle control-transfected H1299 cell lines. (F) Cell apoptosis was determined by flow cytometry after suspension for 24 hours in stable SENP1 knockdown or mock vehicle control-transfected H1299 cell lines. The data are shown as the mean ± SD, *$p < 0.05$, **$p < 0.01$, ***$p < 0.001$.

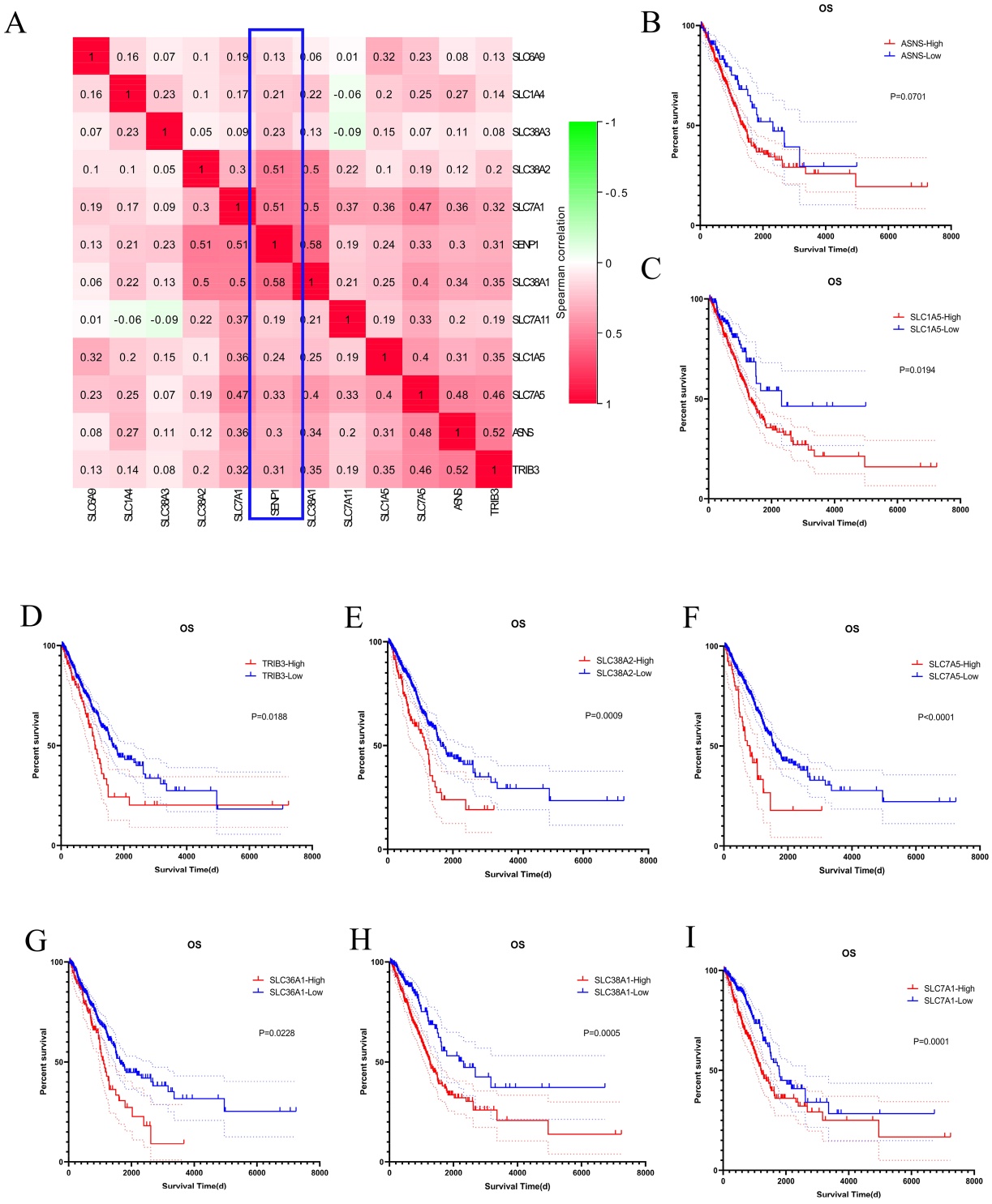

Figure 6

SENP1 expression was significantly correlated with AAR genes expression. (A) Spearmans correlation was used to analyze the correlations the correlation between SENP1 and AAR genes in terms of the expression profile of lung adenocarcinoma from the TCGA database. (B-I) Kaplan–Meier estimates of overall survival according to AAR genes expression in terms of the expression profile of lung adenocarcinoma from the TCGA database.